

JPET #226431

Autophagy Deficiency Diminishes Indomethacin-Induced Intestinal Epithelial Cell Damage through the Activation of ERK/Nrf2/HO-1 Pathway

Satoshi Harada, Takatoshi Nakagawa, Shunichi Yokoe, Shoko Edogawa, Toshihisa
Takeuchi, Takuya Inoue, Kazuhide Higuchi and Michio Asahi

*Department of Internal medicine (II)(S.H., S.E., T.T., T.I., K.H.) and Department of
Pharmacology(T.N., S.Y., M.A.), Faculty of Medicine, Osaka Medical College, Takatsuki,
Osaka, Japan*

JPET #226431

Running title; Amelioration of Indomethacin-induced injury by autophagy deficiency

Corresponding author; Michio Asahi

Department of Pharmacology, Faculty of Medicine, Osaka Medical College, 2-7,

Daigaku-machi, Takatsuki, Osaka 569-8686, Japan

Tel: +81-72-684-6418; Fax:+81-72-684-6518; e-mail: masahi@art.osaka-med.ac.jp

The number of text pages; 28

Number of tables; 1

Number of Figures; 8

Number of References; 39

Number of words in the Abstract; 248

Number of words in the Introduction; 586

Number of words in the Discussion; 993

Abbreviations used; HO-1, heme oxygenase-1; IM, indomethacin; NSAIDs, non-steroidal anti-inflammatory drugs; PPI, proton pump inhibitor; ROS, reactive oxygen species; WT, wild type.

Recommended section; Gastrointestinal, Hepatic, Pulmonary, and Renal

Abstract

Non-steroidal anti-inflammatory drugs (NSAIDs) can cause epithelial cell damage in the stomach, intestine, and colon. NSAIDs are reported to induce autophagy and apoptosis in intestinal epithelial cells; however, their role in cell damage is poorly understood. To examine the role of autophagy in cell damage, we used *Atg5* conditional knocked-out mice (*Atg5*-CKO mice), where the *Atg5* gene is only knocked out in intestinal epithelial cells. In an indomethacin (IM)-induced gastrointestinal ulcer mouse model, intestinal epithelium damage reduced in *Atg5*-CKO mice compared to the damage in wild-type mice. IM-induced damage in IEC6 rat intestinal epithelial cells was reduced when *Atg5* was silenced (IEC6sh*Atg5* cells). Western blot analyses indicated that IM-induced apoptosis decreased, and the potent, oxidative-stress-related signaling pathway ERK/Nrf2/HO-1 was upregulated in IEC6sh*Atg5* cells. An experiment using a reactive oxygen species (ROS)-sensitive fluorescent dye in IEC6sh*Atg5* cells revealed that the amount of ROS under the baselines and the rate of increase after IM treatment were lower than in intact IEC6 cells. The mitochondrial membrane potential under the baselines and the reduction rate in IM-treated IEC6sh*Atg5* cells were lower than in intact IEC6 cells, indicating that autophagy deficiency increased ROS production caused by mitochondrial disturbance. Furthermore, MnTMPyP, an Mn-SOD mimetic, significantly inhibited IM-induced autophagy and subsequent apoptosis, as well as activation of the ERK/Nrf2/HO-1 pathway. These data suggest that autophagy deficiency and subsequent activation of the

JPET #226431

ERK/Nrf2/HO-1 pathway diminished IM-induced, apoptosis-mediated intestinal epithelial cell damage, and genetic analyses of single nucleotide polymorphisms in autophagy-related genes could predict NSAID-induced intestinal injury.

Introduction

Non-steroidal anti-inflammatory drugs (NSAIDs) are known to cause damage such as erosion, hemorrhage, or perforation in the gastric membrane. Recently, capsule endoscopy or balloon enteroscopy revealed that NSAIDs cause membrane damage in not only stomach, but also in the intestine and colon (Graham et al., 2005; Sidhu et al., 2006; Maiden et al., 2007). It has been reported that 68% of patients experience damage in the intestinal membranes at 2 weeks after the internal use of NSAIDs combined with a proton pump inhibitor (PPI) (Maiden et al., 2007). In a Japanese analysis of the frequency of NSAID-induced intestinal ulcer using the database of balloon enteroscopy, intestinal ulceration was observed in about 51% of the patients taking NSAIDs (Matsumoto et al., 2008).

Because the pH is very low in the stomach, antacids such as H₂ receptor antagonists (H₂RA) or PPIs are an efficient treatment of NSAID-induced gastric ulcers (Yeomans et al., 1998). However, antacids may not work in the intestine, because the pH is around 8. In the intestine, NSAIDs reduce ATP production in the mitochondria of intestinal epithelial cells, and therefore the membrane permeability is increased by the resulting disturbance to the maintenance system in the junction between the cells (Bjarnason et al., 1993). Thereby, enteric bacteria, bile acids, and proteases cross the cell membrane, resulting in the migration and activation of neutrophils. The activated neutrophils produce cytokines or nitric oxide, which induces damage in intestinal membranes (Higuchi et al., 2009).

Autophagy plays an important role in maintaining cell homeostasis during nutrient deprivation, oxidative stress, or ER stress (Kuma et al., 2004; Komatsu et al., 2005; Ogata

et al., 2006). Autophagy is induced by the proteins coded by the autophagy-related genes (*Atg*) (Suzuki et al., 2004; Mizushima et al., 2011). The process includes 1) the formation and elongation of isolation membrane, 2) autophagosome formation, 3) docking and fusion with lysosome, and 4) vesicle breakdown or degradation. The Atg12/Atg5 complex, which resides in the isolation membrane, has a pivotal role in membrane elongation, and thus is essential for autophagy. However, an excessive level of autophagy induces non-apoptotic cell death (Chiou et al., 2011). Sulindac sulfide, an NSAID, causes autophagy that induces the death of RGM-1 rat gastric epithelial cells.

Although autophagy and apoptosis are different physiological processes, they have a complicated relationship in terms of their interactions with each other. The activation of autophagy can either promote or inhibit apoptosis depending upon the particular stimulating factors or cell types (Besirli et al., 2011; Saiki et al., 2011). Celecoxib inhibits the proliferation in human gastric cancer cell line, SGC-7901 by the induction of autophagy and subsequent apoptosis (Liu et al., 2014). On the other hand, when apoptosis is activated, autophagy-related proteins such as beclin-1 or Atg5 are degraded by a series of apoptosis-related proteases and caspases, which results in the gradual cessation of autophagy (Luo and Rubinsztein, 2010). Bcl-2 not only functions as an antiapoptotic protein, but also as an antiautophagy protein via its inhibition of beclin-1 (Pattingre et al., 2005).

Knockout of Atg5 in mice (Atg5 KO mice) was lethal to mouse embryos so tissue-specific conditional *Atg5* KO mice have been used to investigate about autophagy *in vivo* (Nakai et al., 2007; Gukovsky and Gukovskaya, 2015). Here, we established intestinal epithelial cell-specific conditional *Atg5* KO mice, and examined whether autophagy may effect

JPET #226431

intestinal epithelial cell damage by an NSAID, indomethacin (IM) *in vivo*. Moreover, *Atg5*-silenced rat intestinal epithelial cells, IEC6shAtg5 cells, were used to reveal the molecular mechanisms underlying the effect of autophagy on IM-induced cell damage.

JPET #226431

Materials and methods

Materials

Antibodies: An anti-PARP1 antibody was purchased from Enzo Life Science Inc.

(Farmingdale, NY). An anti-LC3 antibody was obtained from MBL (Nagoya, Japan).

Anti-total and phospho-ERK antibodies were obtained from CST (Danvers, MA).

Anti-HO-1 and anti-Nrf2 antibodies were from Stressgen Biotech (San Diego, CA) and Santa Cruz Biotech Inc. (Santa Cruz, CA), respectively.

Fluorescent dye: Mitotracker Red CMX ROS was purchased from Life technologies (Carlsbad, CA).

Other reagents: MnTMPyP was procured from Santa Cruz Biotech Inc. (Santa Cruz, CA).

Total ROS/Superoxide Detection Kit was a product of Enzo Life Science Inc. (Farmingdale, NY).

Oral administration of IM and extraction of intestine in WT or *Atg5*-CKO mice

Oral administration of IM was performed as described previously (Tanaka et al., 2002). Briefly, WT and *Atg5*-CKO mice ($n = 5-6$ for each) were given IM p.o. at a dose of 10 mg/kg and killed 24 h later under deep ether anesthesia. The small intestines (stomach to ileum) were excised and used for the measurement of a lesion score or Western blot analyses.

Cell culture

IEC6, a rat intestinal epithelial cell line, was obtained from RIKEN BRC (Saitama, Japan). This cell line was maintained in the growth medium DMEM (Life Technologies, Carlsbad, CA) supplemented with 10% fetal bovine serum, 100 U/mL penicillin, and 100

JPET #226431

µg/mL streptomycin.

IEC6shAtg5 cells (shAtg5 cells), in which the *Atg5* gene was suppressed by shRNA, were maintained in the same medium, except that it was supplemented with 1 µg/mL puromycin (Wako Pure Chemical Industries, Osaka, Japan).

Evaluation of intestinal lesion area and protein expression levels

To evaluate lesion scores, the excised tissues were treated with 2% formalin to fix the tissue walls, opened along the anti-mesenteric attachment, and the area of macroscopically visible lesions was measured under a dissecting microscope with square grids (10×), summed per small intestine, and used as a lesion score. To delineate the damage, 1% Evans blue (Sigma Aldrich, St. Louis, MO) solution was injected i.v. in a volume of 0.5 ml/animal 0.5 h before sacrifice.

For Western blot analyses, the excised tissues were homogenized in lysis buffer (25 mM Tris-HCl, 100 mM NaCl, 1% TritonX-100, 0.25% deoxycholate, pH 7.4) containing protease inhibitor cocktail (Nacalai Tesque, Japan) using a Potter-Elvehjem type homogenizer.

Western blot analysis

Following SDS-PAGE, the gel was put into a semi-dry blotting system (Bio-Rad, Hercules, CA, USA), and the proteins were transferred onto a PVDF membrane (PALL, Port Washington, NY, USA). The membrane was blocked with 5% skimmed milk in PBS containing 0.1% Tween 20 (PBST, blocking buffer), incubated in blocking buffer with the primary antibody of interest, washed three times with PBST, and then incubated with a secondary antibody conjugated with horseradish peroxidase. The membrane was visualized with ImmobilonWestern (Millipore, Hayward, CA, USA), and the image was captured with

JPET #226431

Chemidoc (Bio-Rad, Hercules, CA, USA).

Nrf2 promoter assay

IEC6 cells were transfected with pGL4.37 (ARE/Hygro) and pGL4.74 (hRluc/TK) (Promega, Madison, NY) using Lipofectamine2000 (Life Technologies, Carlsbad, CA). After 48 h, the cells were incubated with indomethacin (IM) with or without MnTMPyP for 5 h. The luciferase activity was measured using Dual-Luciferase Reporter Assay System (Promega, Madison, NY) according to manufacturer's instructions. Chemiluminescence was detected using a GloMax Multi Detection System (Promega, Madison, NY).

Evaluation of cell viability

Cell viability was measured colorimetrically using Cell Counting Kit-8 (Wako Pure Chemical Industries, Osaka, Japan) following the manufacturer's instructions. In brief, cells of interest were plated onto a 96-well plate and incubated overnight to allow the cells to attach. Then, the cells were incubated with or without inhibitors for various periods of time (24–72 h). To measure the daily rate of cell proliferation, the cells were incubated with a WST-8 reagent for 1 h and its absorbance was measured at a wavelength of 450 nm using a microplate reader (Model 680, Bio-Rad, Hercules, CA).

Evaluation of oxidative stress

Total ROS/superoxide Detection kit (Enzo Life Science Inc.) was used to evaluate whether oxidative stress increased in intact and shAtg5 cells before and after IM treatment. Briefly, the cells were plated onto a 96-well plate compatible with fluorescence assay. Twenty-four hours later, the cells were incubated with 200 μ M IM for 1–2 h, which was preincubated for 30 min with or without 5 mM *N*-acetyl cysteine (NAC). Fluorescence was directly measured with GloMax Multi Detection System equipped with an appropriate

JPET #226431

optical kit (blue for ROS, green for Superoxide) (Promega, Madison, NY).

Measurement of mitochondrial membrane potential

Mitochondrial function was estimated using a membrane potential-dependent mitochondria probe, MitoTracker Red CMXRos (Molecular Probe). The cells were pre-incubated with IM for 1 h, after which MitoTracker Red CMXRos was added and further incubation for 1 h was performed. The fluorescence was measured using a 96-well microplate luminometer, GloMax (Promega, Madison, NY).

Results

Evaluation of intestinal epithelial injury in wild-type (WT) and *Atg5*-CKO mice after IM administration.

It was reported that IM induced accumulation of cytoplasmic lipid droplets (LDs), and lipophagy—autophagic degradation of portions of LDs or whole LDs either alone or mixed with other cell contents—was promoted to remove the toxic LDs in IEC6 cells (Narabayashi et al., 2014). To examine how autophagy (including lipophagy) is involved in IM-induced intestinal epithelial injury, we used *Atg5*-CKO mice in which autophagy did not occur only in intestinal epithelial cells. At 24 h after the oral administration of IM to either WT or *Atg5*-CKO mice, they were sacrificed, and the extent of intestinal epithelial injury was evaluated. As a result, the intestinal epithelial injury was significantly decreased in *Atg5*-CKO mice compared to WT mice according to macroscopic finding and ulcer index (Fig. 1A, B).

Evaluation of cell viability in IEC6 or IEC6shAtg5 cells after IM treatment.

To further understand the role of autophagy in intestinal epithelial injury, we established IEC6shAtg5 cells (Fig. 2A) and evaluated them *in vitro*. Cell damage after IM treatment in IEC6shAtg5 cells was significantly increased compared with IEC6 cells, which is consistent with the data *in vivo* (Fig. 1C).

Evaluation of autophagy and apoptosis in IEC6 or IEC6shAtg5 cells after IM treatment.

We retested whether autophagy might occur after IM treatment by carrying out Western blot analyses using an anti-LC3 antibody. The results confirmed that autophagy increased in intact cells after IM treatment, and the increase was totally reversed in IEC6shAtg5 cells

(Fig. 2A).

Next, we evaluated whether apoptosis is related to the decline of cell viability, the cleavage of PARP1, which is the substrate of caspase-3, was evaluated by Western blot analyses. The data showed that the cleavage of PARP1 was significantly suppressed in IEC6shAtg5 cells, indicating that the augmented autophagy after IM treatment might induce apoptosis (Fig. 2B). The subsequent apoptosis is thought to deteriorate the intestinal epithelial cell damages.

Total ROS and superoxide production in IEC6 or IEC6shAtg5 cells.

Autophagy plays an important role in maintaining cell homeostasis during nutrient deprivation, oxidative stress, or ER stress. To examine the mechanism by which autophagy was induced after IM treatment, we focused on oxidative stress. Total ROS and superoxide generation before and after IM treatment were estimated using a Total ROS/superoxide Detection kit (Enzo Life Science Inc.). First, we examined the level of total ROS and superoxide generation in IEC6shAtg5 cells under the baselines. As a result, both total ROS and superoxide generation were significantly increased in IEC6shAtg5 cells compared to intact cells. Second, we examined whether ROS generation was increased after IM treatment in both cells. The data showed that ROS generation were significantly increased in both cells after IM treatment (Fig. 3AB). The elevation of ROS generation was totally reversed by a radical scavenger, *N*-acetylcysteine (NAC). Interestingly, changing rates of relative ROS or superoxide production after IM treatment were significantly different with each other. The changing rate in IEC6shAtg5 cells was significantly lower than in IEC6 cells, indicating that IEC6shAtg5 cells were more tolerated to ROS than IEC6 cells (Fig. 3CD).

Mitochondrial membrane potential before and after IM treatment in IEC6 or IEC6shAtg5 cells.

To reveal the mechanism by which ROS generation were significantly increased in IEC6shAtg5 cells compared to in IEC6 cells at the basal line, and were both significantly increased in both cells after IM treatment, we measured mitochondrial membrane potentials in IEC6 cells and IEC6shAtg5 cells, which is the indicator of mitochondrial activity. If this potential is reduced, it is thought that the percentage of damaged mitochondria might be increased. As a result, the potential was significantly lower in IEC6shAtg5 cells compared with in IEC6 cells at the basal line. IM treatment lowered the potentials in IEC6 cells, but not in IEC6shAtg5 cells (Fig. 4).

Activity of ERK/Nrf2/HO-1 pathway in IEC6 or IEC6shAtg5 cells after IM treatment.

Autophagy is a cytoprotective pathway for degradation of cellular components within autophagic vacuoles caused by various cellular stress.

It was previously reported that heme oxygenase-1 (HO-1) prevented intestinal epithelial cells from IM-induced ulceration in rat. To reveal whether HO-1 is involved in the acquisition of tolerance against ROS in IEC6shAtg5 cells, we examined whether the ERK/Nrf2/HO-1 pathway might be activated in the cells. As shown in Fig. 5AB, ERK phosphorylation and Nrf2/HO-1 expression were upregulated in IEC6shAtg5 cells compared with IEC6 cells. Thus, activation of the ERK/Nrf2/HO-1 pathway could be involved in the acquisition of tolerance against ROS, resulting in the reduction of cell damages in IEC6shAtg5 cells.

Effect of MnTMPyP on the upregulation of autophagy, apoptosis, and ERK/Nrf2/HO-1 pathway after IM treatment in IEC6 cells.

To prove whether ROS regulates IM-induced autophagy and subsequent apoptosis, we used a Mn-SOD mimetic, Mn-TMPyP, to scavenge ROS in a series of experiments and examined the effect of Mn-TMPyP on the cleavage of LC3 or PARP1 after IM treatment. As a result, the upregulation of LC3-II or cleaved PARP1 were totally reversed by Mn-TMPyP (Fig. 6AB). Furthermore, we examined the effect of Mn-TMPyP on IM-induced upregulation of the ERK/Nrf2/HO-1 pathway. The result showed that the upregulation of the pathway was also totally reversed by Mn-TMPyP (Fig. 6C). We also performed Nrf2 promoter analysis to examine the effect of IM with or without Mn-TMPyP on the transcriptional activity, indicating that Nrf2 activity was also upregulated after IM treatment, which was reversed by Mn-TMPyP (Fig. 6D). These results indicates that ROS promoted IM-induced autophagy and subsequent apoptosis, resulting in the intestinal epithelial cell damages, and the damage was strongly blocked by the upregulation of the ERK/Nrf2/HO-1 pathway.

Effect of autophagy deficiency on the ERK/Nrf2/HO-1 pathway in intestinal epithelial cells from WT and *Atg5*-CKO mice.

The ERK/Nrf2/HO-1 pathway was activated to induce the acquisition of tolerance against ROS, resulting in the reduction of cell damages in IEC6shAtg5 cells (Fig.5AB). To confirm whether the pathway may be activated in intestinal epithelial cells from Atg5-CKO mice as well as in IEC6shAtg5 cells, the epithelial cells scraped from the intestines of WT and Atg5-CKO mice with or without IM administration were used for Western blot analyses. As shown in Fig. 7, the ERK/Nrf2/HO-1 pathway in the cells from Atg5-CKO mice was activated compared to those from WT mice without IM administration. Furthermore, the activity was significantly increased after IM treatment only in the cells derived from

JPET #226431

Atg5-CKO mice. These data suggest that the ERK/Nrf2/HO-1 pathway is activated by autophagy deficiency *in vivo*.

Discussion

NSAID-induced gastric membrane damage has been very successfully treated with antacids such as H₂ receptor antagonists (H₂RA) or proton pump inhibitors (PPI) (Yeomans et al., 1998). Given that the pH of intestinal epithelium is neutral—not acidic like the stomach—it is not likely that NSAIDs will be effective, and some reports indicate that they did not ameliorate the damages of intestinal membrane (Daniell, 2012). Thus, in order to treat NSAID-induced intestinal membrane damage, it is very important to elucidate the mechanism.

Since it is reported that autophagy takes place after IM treatment in IEC6 cells as well as apoptosis (Narabayashi et al., 2014), we focused on autophagy, and examined the role of autophagy in intestinal epithelial damage. Here, we showed that prevention of autophagy reduced apoptosis-mediated IM-induced intestinal epithelial cell damage. The amelioration was due to activation of the ERK/Nrf2/HO-1 pathway.

In some contexts, autophagy is regarded as an adaptive response to stress, which promotes survival, whereas in other cases it appears to promote cell death and morbidity (Nakai et al., 2007; Kundu and Thompson, 2008). In our *in vitro* and *in vivo* experiments, prevention of autophagy reduced IM-induced intestinal epithelial cell damage, meaning that autophagy promoted cell death and morbidity. To examine the mechanism, we examined the changes in intracellular signaling pathways before and after IM treatment in IEC6 and IEC6shAtg5 cells. We previously reported that lansoprazole, a PPI, prevented IM-induced intestinal epithelial damage through the upregulation of HO-1 (Yoda et al., 2010). Therefore, we examined whether the potent, oxidative-stress-related signaling pathway, ERK/Nrf2/HO-1 pathway, was upregulated or not. We found that the pathway was more

activated under the baselines and the rate of increase after IM treatment was higher in IEC6shAtg5 cells than in IEC6 cells. This indicates that autophagy deficiency makes the cells more resistant to oxidative stress through activation of the ERK/Nrf2/HO-1 pathway.

The ERK/Nrf2/HO-1 pathway is upregulated by ROS (Papaiahgari et al., 2006; Xu et al., 2013). Since the ERK/Nrf2/HO-1 pathway was activated before and after IM treatment in IEC6shAtg5 cells, it is possible that IEC6shAtg5 cells should produce more ROS than IEC6 cells. Expectedly, ROS production was increased in IEC6shAtg5 cells compared with IEC6 cells. It was revealed that the ROS increase activated ERK, followed by Nrf2 and HO-1 activation. We confirmed this by the fact that activation of the pathway was inhibited by the ROS scavenger MnTMPyP. Together, upregulated ROS production might activate the ERK/Nrf2/HO-1 pathway, resulting in tolerance towards IM-induced oxidative stress. The effects of autophagy deficiency with or without IM treatment on IEC6 cells (*in vitro*) or mouse intestinal epithelial cells (*in vivo*) are summarized in Table 1.

We showed that Nrf2 was activated through the upregulation of ERK phosphorylation before and after IM treatment of IEC6shAtg5 cells. Since it is reported that autophagy deficiency activates Nrf2 through direct interaction between Keap1 and p62 (Lau et al., 2010), Nrf2 might be activated by two ways, the upregulation of ERK phosphorylation and the inhibition of Keap1-mediated degradation. Nrf2 activation functions as a potent cell survival factor by the induction of not only antioxidative enzymes such as HO-1, but also detoxifying enzymes such as GSTM1 (Chowdhry et al., 2013). Therefore, Nrf2 activation might be the most important factor in terms of the protective effect after IM treatment in IEC6shAtg5 cells.

Autophagy normally recycles macro-molecular aggregates produced through

oxidative-stress mediated pathways, and also may reduce the mitochondrial production of reactive oxygen species through recycling of old and damaged mitochondria (Hensley and Harris-White, 2015). Thus, autophagy is thought to be an essential cellular antioxidant pathway (Giordano et al., 2014). In our experiment, IEC6shAtg5 cells where autophagy did not occur produced more ROS than IEC6 cells. The increase of ROS production in autophagy deficient cells might be because autophagy mainly reduces oxidative stress by degrading dysfunctional mitochondria, which releases ROS.

We found that IM-induced intestinal epithelial cell damage might be mediated by ROS production, followed by a decrease in mitochondrial membrane potential (Chung et al., 2003). Decreased mitochondrial membrane potential is thought to induce ROS production (Hosseini et al., 2014). Since the increase in ROS, which results from decreased mitochondrial membrane potential, induced disturbance of mitochondrial membranes, it is likely that IM-induced ROS production took the form of a vicious cycle. This cycle might result in the deterioration of oxidative stress, leading to apoptosis.

Here, we demonstrated that autophagy deficiency diminishes IM-induced intestinal epithelial cell damage through activation of the ERK/Nrf2/HO-1 pathway. This does not simply mean that autophagy deteriorates IM-induced intestinal epithelial cell damage. Since autophagy is primarily a protective process for the cell, autophagy deficiency may not be protective in a different situation. If oxidative stress is increased and ROS production is harmful to the cells, autophagy deficiency will not be protective. Although oxidative stress was increased in IEC6shAtg5 cells under the baselines, the amount of ROS might not be harmful to the cells; instead, the ROS level could make the cells resistant toward oxidative stress. Furthermore, the data may also indicate that individuals with an autophagy-related

JPET #226431

disorder such as Crohn's disease (Scharl et al., 2012; Spalinger et al., 2014) or with a functional variant of the autophagy-related gene, *ATG*, (Latiano et al., 2008; Martin et al., 2012; Kimura et al., 2014) are resistant towards NSAID-induced intestinal epithelial cell damage. Genetic analyses of single nucleotide polymorphisms in *ATG* genes could be used to predict NSAID-induced intestinal injury.

In summary, we revealed that IM-induced intestinal epithelial cells were damaged by oxidative stress due to mitochondrial dysfunction. The cell damage was partly caused by apoptosis. In a condition where autophagy does not function, the cell damage was reduced through activation of the ERK/Nrf2/HO-1 pathway. The possible mechanism by which autophagy deficiency diminishes IM-induced intestinal epithelial cell damage was designated in Fig. 8. Oxidative stress might be one of the most important factors inducing IM-induced intestinal epithelial cell damage. Activation of anti-oxidative signaling systems such as the ERK/Nrf2/HO-1 pathway could be very effective to prevent small intestine from IM-induced injury.

JPET #226431

Authorship Contributions

Participated in research design: Nakagawa, Higuchi, and Asahi.

Conducted experiments: Harada, Nakagawa, and Yokoe.

Contributed new reagents or analytic tools: Nakagawa, Edogawa, Takeuchi, and Inoue.

Performed data analysis: Harada, Nakagawa, Higuchi, and Asahi.

Wrote or contributed to the writing of the manuscript: Asahi.

References

- Besirli CG, Chinskey ND, Zheng QD and Zacks DN (2011) Autophagy activation in the injured photoreceptor inhibits fas-mediated apoptosis. *Invest Ophthalmol Vis Sci* **52**:4193-4199.
- Bjarnason I, Hayllar J, MacPherson AJ and Russell AS (1993) Side effects of nonsteroidal anti-inflammatory drugs on the small and large intestine in humans. *Gastroenterology* **104**:1832-1847.
- Chiou SK, Hoa N and Hodges A (2011) Sulindac sulfide induces autophagic death in gastric epithelial cells via survivin down-regulation: a mechanism of NSAIDs-induced gastric injury. *Biochem Pharmacol* **81**:1317-1323.
- Chowdhry S, Zhang Y, McMahon M, Sutherland C, Cuadrado A and Hayes JD (2013) Nrf2 is controlled by two distinct beta-TrCP recognition motifs in its Neh6 domain, one of which can be modulated by GSK-3 activity. *Oncogene* **32**:3765-3781.
- Chung YM, Bae YS and Lee SY (2003) Molecular ordering of ROS production, mitochondrial changes, and caspase activation during sodium salicylate-induced apoptosis. *Free Radic Biol Med* **34**:434-442.
- Daniell HW (2012) NSAID-PPI enteropathy in humans. *Gastroenterology* **142**:e20; author reply e20-21.
- Giordano S, Darley-Usmar V and Zhang J (2014) Autophagy as an essential cellular antioxidant pathway in neurodegenerative disease. *Redox Biol* **2**:82-90.
- Graham DY, Opekun AR, Willingham FF and Qureshi WA (2005) Visible small-intestinal mucosal injury in chronic NSAID users. *Clin Gastroenterol Hepatol* **3**:55-59.
- Gukovsky I and Gukovskaya AS (2015) Impaired autophagy triggers chronic pancreatitis: lessons from pancreas-specific atg5 knockout mice. *Gastroenterology* **148**:501-505.
- Hensley K and Harris-White ME (2015) Redox regulation of autophagy in healthy brain and neurodegeneration. *Neurobiol Dis*.
- Higuchi K, Umegaki E, Watanabe T, Yoda Y, Morita E, Murano M, Tokioka S and Arakawa T (2009) Present status and strategy of NSAIDs-induced small bowel injury. *J Gastroenterol* **44**:879-888.
- Hosseini MJ, Shaki F, Ghazi-Khansari M and Pourahmad J (2014) Toxicity of copper on isolated liver mitochondria: impairment at complexes I, II, and IV leads to increased ROS production. *Cell Biochem Biophys* **70**:367-381.
- Kimura T, Watanabe E, Sakamoto T, Takasu O, Ikeda T, Ikeda K, Kotani J, Kitamura N, Sadahiro T, Tateishi Y, Shinozaki K and Oda S (2014) Autophagy-related IRGM polymorphism is associated with mortality of patients with severe sepsis. *PLoS One* **9**:e91522.
- Komatsu M, Waguri S, Ueno T, Iwata J, Murata S, Tanida I, Ezaki J, Mizushima N, Ohsumi Y, Uchiyama Y, Kominami E, Tanaka K and Chiba T (2005) Impairment of starvation-induced and constitutive autophagy in Atg7-deficient mice. *J Cell Biol* **169**:425-434.
- Kuma A, Hatano M, Matsui M, Yamamoto A, Nakaya H, Yoshimori T, Ohsumi Y, Tokuhisa T and Mizushima N (2004) The role of autophagy during the early neonatal starvation period. *Nature* **432**:1032-1036.
- Kundu M and Thompson CB (2008) Autophagy: basic principles and relevance to disease. *Annu Rev Pathol* **3**:427-455.
- Latiano A, Palmieri O, Valvano MR, D'Inca R, Cucchiara S, Riegler G, Staiano AM, Ardizzone S, Accomando S, de Angelis GL, Corritore G, Bossa F and Annese V (2008) Replication of

- interleukin 23 receptor and autophagy-related 16-like 1 association in adult- and pediatric-onset inflammatory bowel disease in Italy. *World J Gastroenterol* **14**:4643-4651.
- Lau A, Wang XJ, Zhao F, Villeneuve NF, Wu T, Jiang T, Sun Z, White E and Zhang DD (2010) A noncanonical mechanism of Nrf2 activation by autophagy deficiency: direct interaction between Keap1 and p62. *Mol Cell Biol* **30**:3275-3285.
- Liu M, Li CM, Chen ZF, Ji R, Guo QH, Li Q, Zhang HL and Zhou YN (2014) Celecoxib regulates apoptosis and autophagy via the PI3K/Akt signaling pathway in SGC-7901 gastric cancer cells. *Int J Mol Med* **33**:1451-1458.
- Luo S and Rubinsztein DC (2010) Apoptosis blocks Beclin 1-dependent autophagosome synthesis: an effect rescued by Bcl-xL. *Cell Death Differ* **17**:268-277.
- Maiden L, Thjodleifsson B, Seigal A, Bjarnason, II, Scott D, Birgisson S and Bjarnason I (2007) Long-term effects of nonsteroidal anti-inflammatory drugs and cyclooxygenase-2 selective agents on the small bowel: a cross-sectional capsule enteroscopy study. *Clin Gastroenterol Hepatol* **5**:1040-1045.
- Martin LJ, Gupta J, Jyothula SS, Butsch Kovacic M, Biagini Myers JM, Patterson TL, Ericksen MB, He H, Gibson AM, Baye TM, Amirisetty S, Tsoras AM, Sha Y, Eissa NT and Hershey GK (2012) Functional variant in the autophagy-related 5 gene promoter is associated with childhood asthma. *PLoS One* **7**:e33454.
- Matsumoto T, Kudo T, Esaki M, Yano T, Yamamoto H, Sakamoto C, Goto H, Nakase H, Tanaka S, Matsui T, Sugano K and Iida M (2008) Prevalence of non-steroidal anti-inflammatory drug-induced enteropathy determined by double-balloon endoscopy: a Japanese multicenter study. *Scand J Gastroenterol* **43**:490-496.
- Mizushima N, Yoshimori T and Ohsumi Y (2011) The role of Atg proteins in autophagosome formation. *Annu Rev Cell Dev Biol* **27**:107-132.
- Nakai A, Yamaguchi O, Takeda T, Higuchi Y, Hikoso S, Taniike M, Omiya S, Mizote I, Matsumura Y, Asahi M, Nishida K, Hori M, Mizushima N and Otsu K (2007) The role of autophagy in cardiomyocytes in the basal state and in response to hemodynamic stress. *Nat Med* **13**:619-624.
- Narabayashi K, Ito Y, Eid N, Maemura K, Inoue T, Takeuchi T, Otsuki Y and Higuchi K (2014) Indomethacin suppresses LAMP-2 expression and induces lipophagy and lipoapoptosis in rat enterocytes via the ER stress pathway. *J Gastroenterol*.
- Ogata M, Hino S, Saito A, Morikawa K, Kondo S, Kanemoto S, Murakami T, Taniguchi M, Tani I, Yoshinaga K, Shiosaka S, Hammarback JA, Urano F and Imaizumi K (2006) Autophagy is activated for cell survival after endoplasmic reticulum stress. *Mol Cell Biol* **26**:9220-9231.
- Papiahgari S, Zhang Q, Kleeberger SR, Cho HY and Reddy SP (2006) Hyperoxia stimulates an Nrf2-ARE transcriptional response via ROS-EGFR-PI3K-Akt/ERK MAP kinase signaling in pulmonary epithelial cells. *Antioxid Redox Signal* **8**:43-52.
- Pattingre S, Tassa A, Qu X, Garuti R, Liang XH, Mizushima N, Packer M, Schneider MD and Levine B (2005) Bcl-2 antiapoptotic proteins inhibit Beclin 1-dependent autophagy. *Cell* **122**:927-939.
- Saiki S, Sasazawa Y, Imamichi Y, Kawajiri S, Fujimaki T, Tanida I, Kobayashi H, Sato F, Sato S, Ishikawa K, Imoto M and Hattori N (2011) Caffeine induces apoptosis by enhancement of autophagy via PI3K/Akt/mTOR/p70S6K inhibition. *Autophagy* **7**:176-187.
- Scharl M, Mwinyi J, Fischbeck A, Leucht K, Eloranta JJ, Arikkat J, Pesch T, Kellermeier S, Mair A, Kullak-Ublick GA, Truninger K, Noreen F, Regula J, Gaj P, Pittet V, Mueller C, Hofmann C, Fried M, McCole DF and Rogler G (2012) Crohn's disease-associated polymorphism within the PTPN2 gene affects muramyl-dipeptide-induced cytokine secretion and autophagy. *Inflamm Bowel Dis* **18**:900-912.
- Sidhu R, Sanders DS, McAlindon ME and Kapur K (2006) Capsule endoscopy for the evaluation

JPET #226431

- of nonsteroidal anti-inflammatory drug-induced enteropathy: United Kingdom pilot data. *Gastrointest Endosc* **64**:1035.
- Spalinger MR, Rogler G and Scharl M (2014) Crohn's disease: loss of tolerance or a disorder of autophagy? *Dig Dis* **32**:370-377.
- Suzuki K, Noda T and Ohsumi Y (2004) Interrelationships among Atg proteins during autophagy in *Saccharomyces cerevisiae*. *Yeast* **21**:1057-1065.
- Tanaka A, Hase S, Miyazawa T, Ohno R and Takeuchi K (2002) Role of cyclooxygenase (COX)-1 and COX-2 inhibition in nonsteroidal anti-inflammatory drug-induced intestinal damage in rats: relation to various pathogenic events. *J Pharmacol Exp Ther* **303**:1248-1254.
- Xu Y, Duan C, Kuang Z, Hao Y, Jeffries JL and Lau GW (2013) *Pseudomonas aeruginosa* pyocyanin activates NRF2-ARE-mediated transcriptional response via the ROS-EGFR-PI3K-AKT/MEK-ERK MAP kinase signaling in pulmonary epithelial cells. *PLoS One* **8**:e72528.
- Yeomans ND, Tulassay Z, Juhasz L, Racz I, Howard JM, van Rensburg CJ, Swannell AJ and Hawkey CJ (1998) A comparison of omeprazole with ranitidine for ulcers associated with nonsteroidal antiinflammatory drugs. Acid Suppression Trial: Ranitidine versus Omeprazole for NSAID-associated Ulcer Treatment (ASTRONAUT) Study Group. *N Engl J Med* **338**:719-726.
- Yoda Y, Amagase K, Kato S, Tokioka S, Murano M, Kakimoto K, Nishio H, Umegaki E, Takeuchi K and Higuchi K (2010) Prevention by lansoprazole, a proton pump inhibitor, of indomethacin -induced small intestinal ulceration in rats through induction of heme oxygenase-1. *J Physiol Pharmacol* **61**:287-294.

JPET #226431

Footnotes

This study was supported, in part, by a grant-in-Aid for Scientific Research (C) no. 25460397 from the Japan Society for the Promotion of Science (M.A) by the Ministry of Education, Science, Culture, Sports and Technology, Japan.

To whom correspondence should be addressed: Michio Asahi; Tel: +81-72-684-6418; Fax:+81-72-684-6518; e-mail; masahi@art.osaka-med.ac.jp

JPET #226431

Table 1. Effect of autophagy deficiency with or without IM treatment on IEC6 cells or mouse intestinal epithelial cells.

	Epithelial cell damage	Autophagy	Apoptosis	Oxidative stress	ERK/Nrf2/HO-1
WT	-	+	+	+	+
WT +IM	+++	+++	+++	+++	++
Atg-KO	-	-	+	++	++
Atg-KO +IM	+	-	++	+++	+++

Legends to figures

Fig. 1. Role of Atg5 in the injury of small intestine after IM treatment in vitro and in vivo.

(A) Gross appearance of intestinal lesions and (B) the ulcer index after IM administration in WT and conditional Atg5KO mice. The arrows indicate epithelial erosion caused by IM-induced intestinal injuries. The values of ulcer index are expressed as the mean \pm SE. ($n = 5$). The statistical analysis was performed with Tukey's method. (*; $P < 0.05$) (C) The cytotoxicity was estimated after the treatment with various concentrations of IM in IEC6 and IEC6shAtg5 cells. Open bar; IEC6 cells, closed bar; IEC6shAtg5 cells. The statistical analysis was performed using Tukey's method. (*; $P < 0.05$)

Fig. 2. Induction of autophagy and subsequent apoptosis by IM treatment in IEC6 cells, not in IEC6shAtg5 cells.

The cells were treated with various durations (0, 1, 2, 4, 8, 12 h) of 200 μ M IM. (A) LC3 expression levels at each timing in IEC6 cells and IEC6shAtg5 cells were determined using Western blot analyses. Arrow and arrowhead indicate LC3-I and LC3-II, respectively. (B) The cleavage of PARP1 in IM-treated IEC6 cells and IEC6shAtg5 cells was determined. Arrow and arrowhead indicate intact and cleaved PARP1, respectively.

Fig. 3. ROS generation before and after IM treatment in IEC6 and IEC6shAtg5 cells.

(A, B) Both total ROS and superoxide were estimated before and after the treatment of 200 μ M IM in IEC6 and IEC6shAtg5 cells using a Total ROS/superoxide Detection kit

(Enzo Life Science Inc.). The effect of *N*-acetyl cysteine (NAC) was evaluated to confirm that the assay was suitable ($*P < 0.05$). (C, D) The changing rates of relative ROS or superoxide production after various concentrations (0, 50, 100, 200 μ M) of IM treatment were estimated in both cells and compared with each other. ($*P < 0.05$; $**P < 0.01$)

Fig. 4. Quantitative evaluation of functionally active mitochondria before and after IM treatment in IEC6 cells and IEC6shAtg5 cells.

(A) Mitochondria staining with MitoTracker Red CMXRos, a membrane potential dependent mitochondria probe. Cells were pre-incubated with or without 200 μ M IM for 1 h; then, MitoTracker Red CMXRos was added, and further incubated for 1 h. The fluorescence was measured using GloMax (Promega). $*P < 0.05$; Tukey's test. (B) The rate of decrease in functionally active mitochondria before and after IM treatment in IEC6 and IEC6shAtg5 cells. The fluorescence of IM-treated cells was divided with that of control cell. $**P < 0.01$; Mann-Whitney U-Test.

Fig. 5. Changes of protein expression levels after IM treatment in IEC6 and IEC6shAtg5 cells.

The cells were treated with 200 μ M IM for the indicated times. The protein expression levels of total and phosphorylated ERK (A), Nrf2, and HO-1 (B) at each time after IM treatment in IEC6 and IEC6shAtg5 cells were determined using Western blot analyses.

Fig. 6. Involvement of ROS in IM-induced autophagy (A), subsequent apoptosis (B), and ERK/Nrf2/HO-1 pathway (C, D).

After the preincubation with or without 10 μ M MnTMPyP for 30 min, IEC6 cells were treated with 200 μ M IM for another 2 h. The cleavage of LC3 (A) or PARP1 (B) were determined using Western blot analyses. Arrow indicates LC3-I (A) or intact PARP1 (B),

JPET #226431

and arrowhead indicates LC3-II (A) or cleaved PARP1 (B). (C) Using the same samples, the levels of ERK phosphorylation, Nrf2 stabilization and HO-1 induction were determined using Western blot analyses. (* $p < 0.01$) (D) After the preincubation with or without 1 μ M MnTMPyP for 30 min, IEC6 cells were treated with 200 μ M IM for another 2 h. Nrf2 promoter activity was evaluated by a luciferase assay.

Fig. 7. Effects of autophagy deficiency and IM administration on the ERK/Nrf2/HO-1 pathway in small intestinal mucosa.

WT and Atg5 KO mice were treated with or without IM administration orally. After 24h, small intestines (stomach to ileum) of the sacrificed animals were excised, and the mucosa were surgically scraped. The scraped tissues were collected and analyzed with Western blot analyses. (* $p < 0.05$)

Fig. 8. Possible mechanism for the amelioration of IM-induced intestinal epithelial cell injury by autophagy deficiency.

(A) In normal cells, oxidative stress is suppressed by autophagy and, therefore, the ERK/Nrf2/HO-1 pathway is not activated under basal conditions. After IM treatment, the cells cannot fully prevent apoptosis-induced cell damage due to the increase of oxidative stress.

(B) In autophagy-deficient cells, the ERK/Nrf2/HO-1 pathway is activated by oxidative stress even under basal conditions. The cells can minimize apoptosis-induced cell damage after IM treatment, because it is more resistant to oxidative stress due to the upregulated ERK/Nrf2/HO-1 pathway.

Fig. 1.

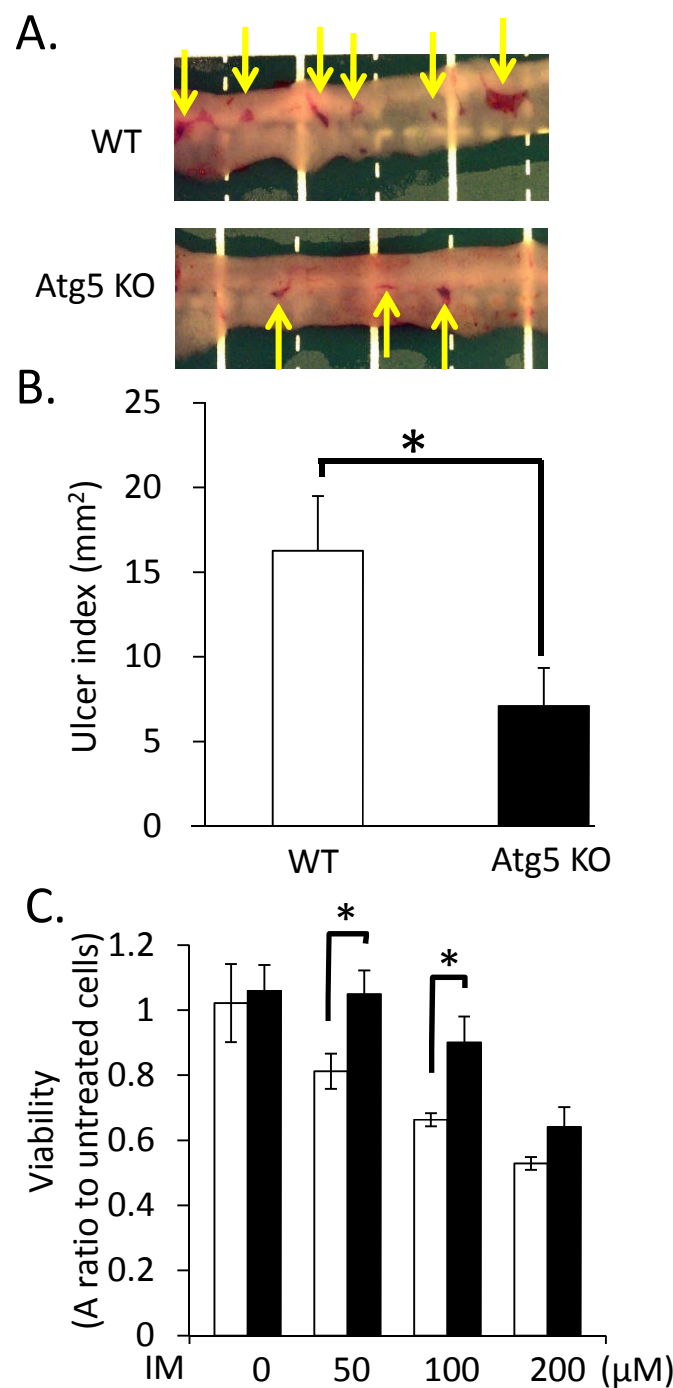


Fig. 2.

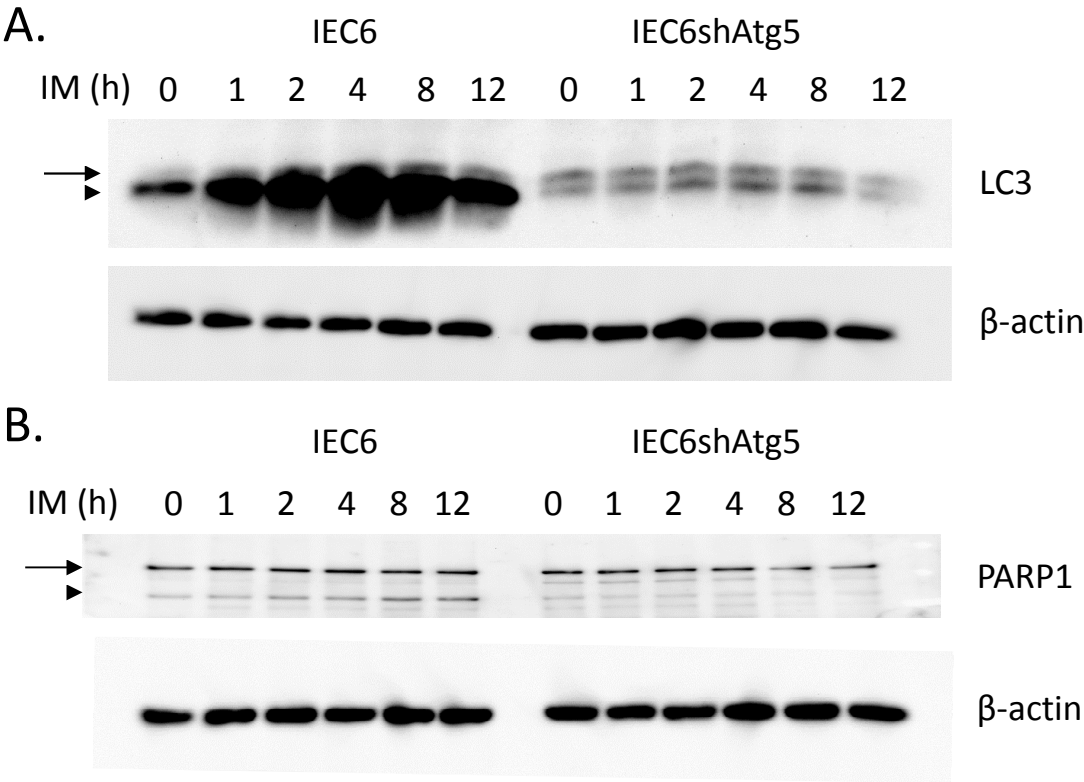


Fig. 3.

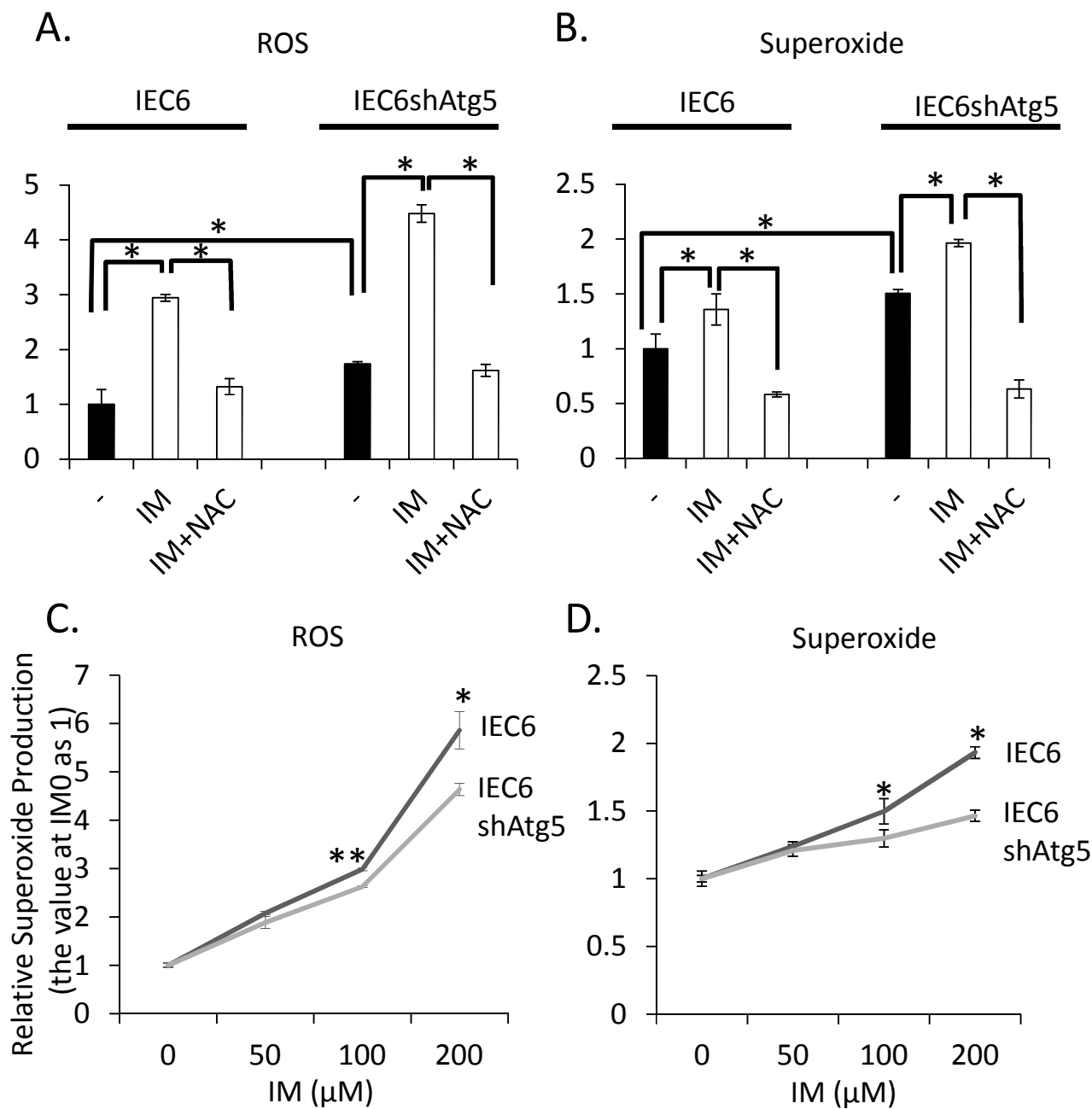


Fig. 4.

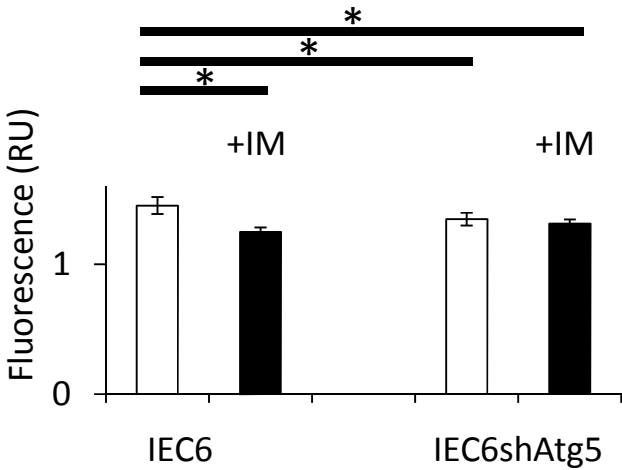


Fig. 5.

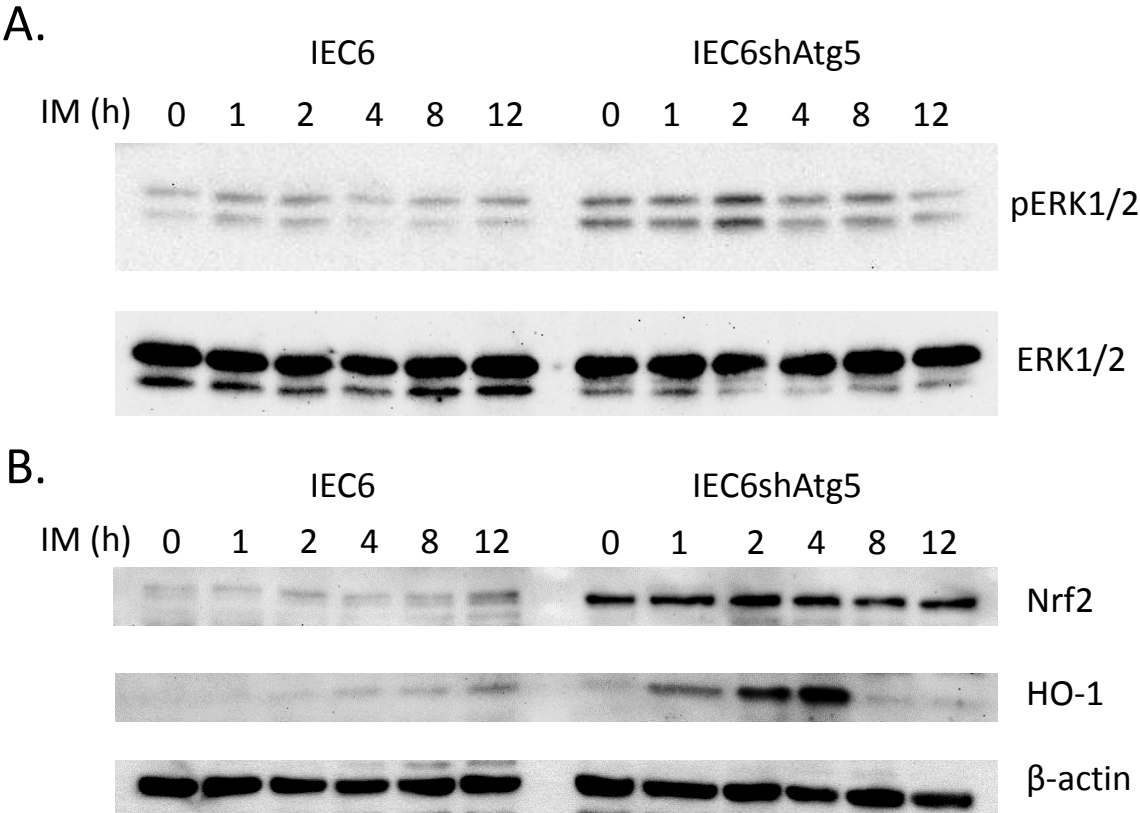


Fig. 6.

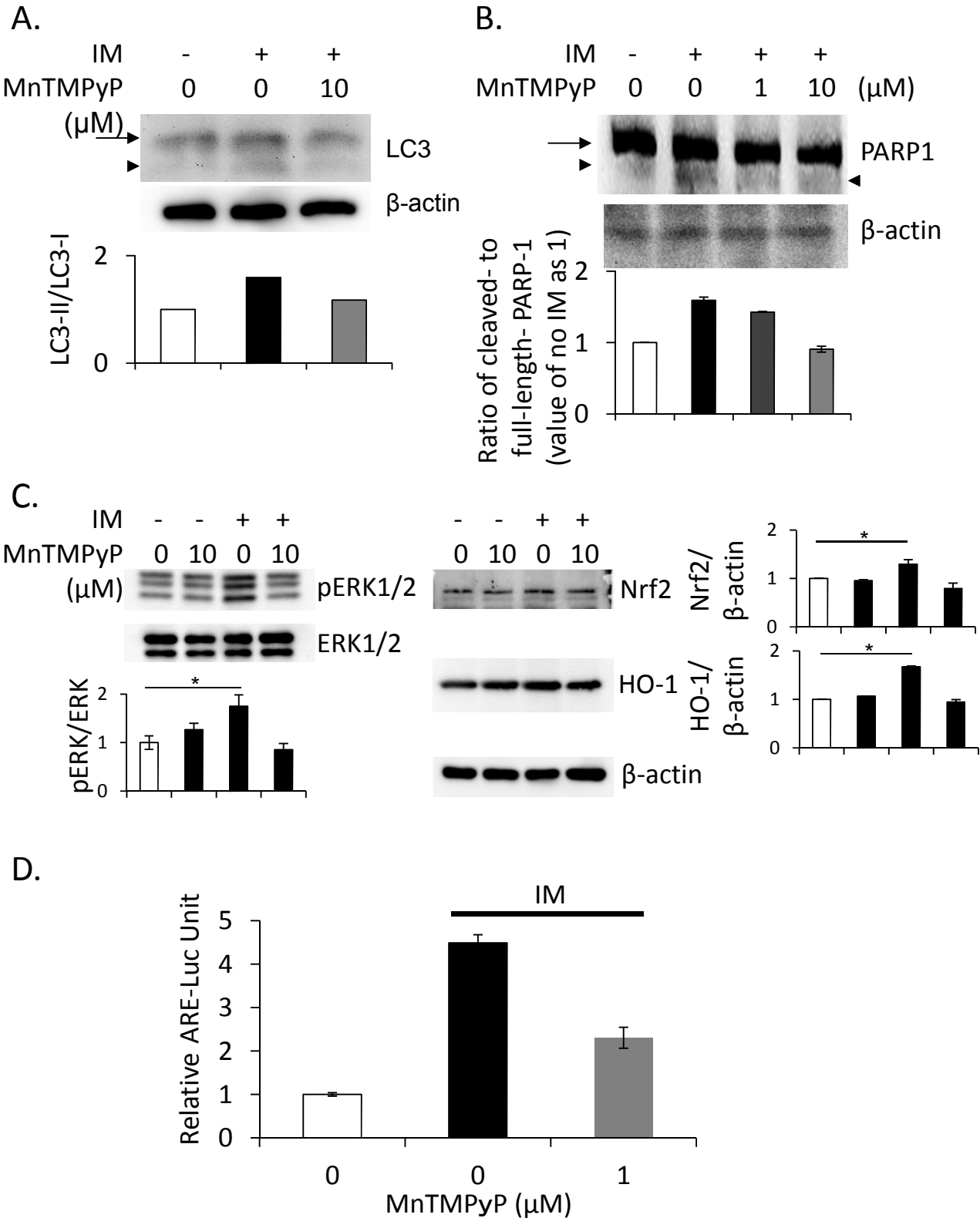


Fig. 7.

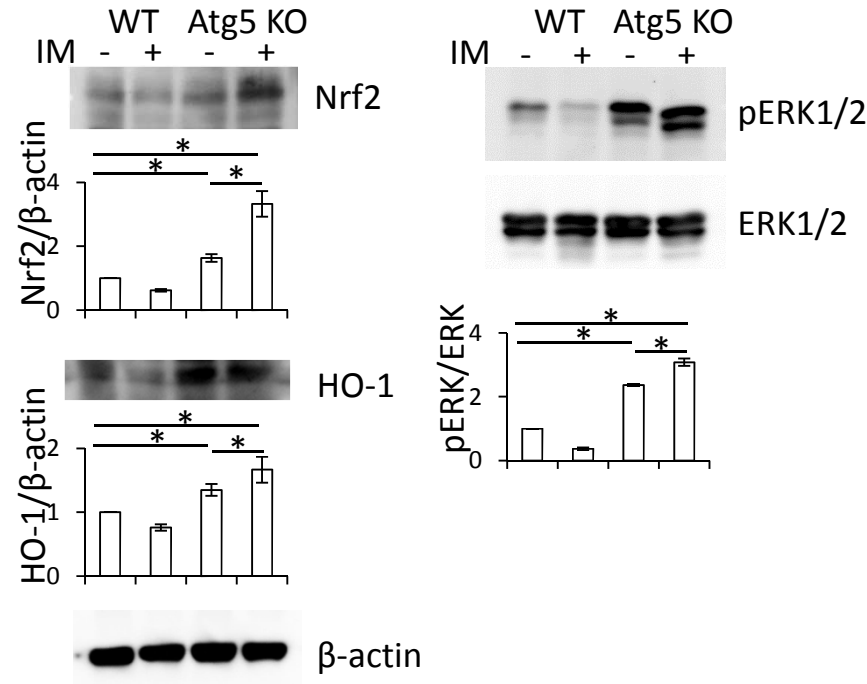
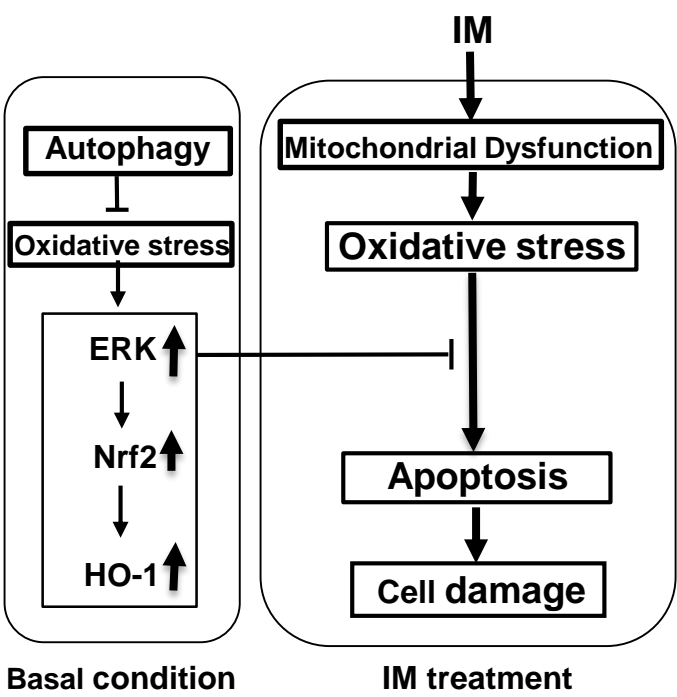


Fig. 8.

A. Normal cells



B. Autophagy-deficient cells

